Title: Permanent human occupation of the central Tibetan Plateau in the Early Holocene

Authors: M.C. Meyer,[1,*] M.S. Aldenderfer,[2,*] Z. Wang,[1] D.L. Hoffmann,[3] J.A. Dahl,[4] D. Degering,[5] W.R. Haas,[6] F. Schlütz[7]

Affiliations:

[1] University of Innsbruck, Institute for Geology, 6020 Innsbruck, Austria

[2] School of Social Sciences, Humanities, and Arts, University of California, Merced, CA 95343, USA

[3] Department of Human Evolution, Max Planck Institute for Evolutionary Anthropology, D-04103 Leipzig, Germany

[4] National Isotope Centre, GNS Science, Lower Hutt 5040, New Zealand

[5] ADD ideas Albrecht und Detlev Degering GbR, Zum Erzengel Michael 19, 01723 Mohorn, Germany

[6] Department of Anthropology, University of Wyoming, Laramie, WY 82071, USA

[7] Lower Saxony Institute for Historical Coastal Research, Wilhelmshaven, Germany

* Corresponding authors

One sentence summary: ^{230}Th/U, luminescence and ^{14}C dating support the presence of a pre-agricultural occupation of the high elevation central Tibetan Plateau.

Abstract: Current models of the peopling of the higher elevation zones of the Tibetan Plateau postulate that permanent occupation could only be facilitated by an agricultural lifeway at ca. 3.6 thousand calibrated ^{14}C years before present (ka cal. BP). Here we report on a re-analysis of the chronology of the Chusang site, located on the central Tibetan Plateau at an elevation of ~4270 meters asl. The minimum age of the site is fixed at ca. 7.4 ka (^{230}Th/U dating) with a maximum age between ca. 8.20-12,67 ka cal. BP (^{14}C assays). Travel cost modelling and archaeological data suggest the site was part of an annual, permanent, pre-agricultural occupation of the central plateau. These findings challenge current models of the occupation of the Tibetan Plateau.

Main text:

The nature and timing of a permanent human settlement on the Tibetan Plateau and the accompanying cultural and physiological responses, including genetic adaptations, that facilitate life at high altitude, are subject to ongoing debate *(1-5)*. Tibet forms the high altitude core of Asia (Fig. 1) and while access to the north-eastern fringes of the plateau from the adjacent North Asian lowlands via the Yellow river and the Qinghai basin is relatively easy, venturing into the core of the plateau, with elevations well above 4000 m above sea level (masl) and cold, arid and periglacial conditions, is considerably more challenging. Permanent human occupation of the Tibetan Plateau was thus impeded by the combined effect of remoteness, low primary productivity, and topography as well as the physiological constraints of cold stress and hypoxia *(6)*. Furthermore, the climatic and paleoenvironmental constraints on this colonisation process are poorly understood *(7-9)*. The number of chronometrically-dated archaeological sites remains small, and most of them are located on the north-eastern margin of the plateau *(1, 7, 10)*. Most of these sites, ranging in date from ca. 9-15 ka cal. BP, are at medium to low elevations (≤ 3300 masl), and are believed to have been short-term, seasonal occupations monitored from lower elevation base camps *(7, 10)*.

Current archaeological models that address the timing of a permanent occupation on the high elevation step of the plateau postulate that it could only have been facilitated by the advent of an agropastoral economy, perhaps as early as ca. 5.2 ka cal. BP, and more certainly, with the establishment of permanent villages fully reliant upon agriculture, by ca. 3.6 ka cal. BP *(1, 4, 5)*. The presence of securely dated, pre-5.2 ka sites from the interior, high-elevation step of the plateau would challenge these models and would be consistent with research on the human genetics of modern plateau peoples, which postulates the presence of a permanent population on the high central plateau dating by at least 8.0-8.4 ka ago and possibly as early as the Late Paleolithic *(11-15)*.

Here we report the results of an extensive re-analysis of the geochronology, paleoenvironment, and archaeology of the Chusang site, which is located on the central plateau ~80 km northwest of Lhasa at an elevation of ~4270 masl near Chusang, a village known for its hydrothermal springs and extensive travertine formations (Fig. 1). The site, discovered in 1998, consists of 19 human hand and footprints found on the surface of a fossil travertine (i.e. a spring carbonate deposited from hydrothermal water) that formed when hot spring discharge was significantly higher compared to today *(16-18)* (text S1; Fig. S1). Size variation in the prints suggests that up to six individuals, including possibly two children, created them. Optically stimulated luminescence (OSL) dating of quartz grains extracted from the travertine suggested that the imprints were created at ca. 20 ka, making Chusang the only archaeological site from the interior of the plateau for which a Paleolithic age assignment is based on a chronometric date *(16)*. However, the complex sedimentological and dosimetric setting at Chusang raises the possibility that the luminescence chronology is severely flawed *(7, 8)*.

Although there are other archaeological sites on the interior of the plateau of reputed Paleolithic age, all are stone tool assemblages of surface finds *(7, 10)* and none has been directly chronometrically dated. The lack of securely dated early sites on the central plateau makes a reanalysis of the chronology of Chusang relevant to a reassessment of current models of the peopling of the Tibetan plateau (Fig. 1).

The hand and footprints are scattered over an area of ~20 by 30 m and occur at the surface of a single sheet of travertine *(16)* (Fig. S1). This sheet is up to 1 m thick, extends for several tens of meters further to the east and is underlain by colluvium (Figs. 2, S2 and S3). The imprints are between 2 and 7 mm deep and the anatomical details of human hands and feet are well preserved (Fig. 3). The imprints were not engraved into the travertine as evidence for pecking, scratching, or carving is absent, but must have formed at a very early stage of hydrothermal carbonate formation (probably within a few months after calcite precipitation), when the top layer of the travertine was still soft and deformable under the weight of a human body. This mechanism is supported by petrographic evidence suggesting that the annual travertine layers from directly below these imprints are continuous but bended *(17)* (Fig. 3C, text S1). A chronometric age for the travertine that carries the imprints will therefore constrain the time of human presence at these hydrothermal springs.

A thorough understanding of the sedimentology and petrology of the Chusang travertine in tandem with the application of multiple dating techniques is key to developing an accurate chronology for the travertine and the embedded hand and footprints, and also important for explaining their formation and preservation *(18)*. The travertine is a fossil spring deposit with a total thickness of ~24 m. The upper ~11 m of the section are characterized by porous, detrital rich travertine sheets that are up to two meters in thickness and laterally extensive (Figs. 2 and S2). Numerous layers of colluvium (i.e. debris flows that originated from the adjacent hill slopes, labelled as diamict massive stratified (Dms) #1 to #4 in Figs. 2 and S2) are intercalated into this upper travertine section. These colluvial

layers are typically 0.5 to 2 meters in thickness and can contain (mostly microscopic) organic material. Sedimentology and thin section microscopy (text S1, Figs. S4 and S5) show that the travertine sheets (including the imprinted travertine) are (i) annually layered on the cm-scale (composed of porous summer and dense winter layers), (ii) often show clastic micro-fabrics (e.g. clasts of re-deposited travertine), (iii) reveal micro-fabrics that are typical for hydrothermal spring carbonates (dendritic crystals) and (iv) precipitated synchronous with clastic sediment input (debris flows) from the hill slopes. Many of these fabrics show evidence for recrystallization. In contrast to this detrital rich travertine-colluvium succession, relatively dense and clean cements are encountered in the pore spaces of the imprinted travertine (Fig. 3C).

A total of 11 samples (nine travertine and two colluvium samples) were collected from the upper travertine section for ^{230}Th/U, OSL and radiocarbon dating as well as for palynological analysis (Fig. S1). Of the nine travertine samples three were retrieved directly adjacent to imprints, two from the same stratigraphic horizon as the imprints, while the remaining four samples are from stratigraphic deeper levels. The two colluvium samples were collected from stratigraphic positions directly below and 8.2 m below the imprinted travertine sheet (see Fig. S1 for sampling locations). The details of each dating method are discussed in the material and method supplement *(19)* and summarized into one chronology (Fig. 2).

Travertine is in principle amenable to ^{230}Th/U dating but the high detrital content and diagenetic alteration (recrystallization) of the Chusang travertine impedes routine dating. Hence, we followed a modified dating protocol and mapped and sub-sampled individual (preferentially primary and dense) micro-fabrics to minimise the risk of sampling altered, potentially recrystallised carbonate *(19)*. We used an isochron approach to account for significant and variable detrital contamination. Multiple sub-samples can also help to identify potential problems arising from open system behaviour. Where thick enough, clean and dense pore cements were targeted for ^{230}Th/U dating as well. The three ^{230}Th/U isochron ages from the travertine sheet that carries the human imprints have very low precision (typically 50% relative error and larger) and the isochron plots indicate more than two isotopic endmembers (Table S1). We conclude that, despite our attempt to sample single mineral phases, the intergrowth of different crystal micro-fabrics and/or recrystallization (potentially entailing open system behaviour) have had severe impacts on the isotopic system and thus have hampered our ability to retrieve ^{230}Th/U ages of acceptable precision. Nevertheless, all isochron plots (i) broadly confirm bulk earth values for the initial ^{238}U/^{232}Th activity ratio and (ii) return early Holocene ages (average of 10.3 ka), pointing towards a certain degree of consistency in the ^{230}Th/U isochron data *(19)*. The ^{230}Th/U ages from different types of pore cements obtained on the same samples are typically more precise and vary from ca. 5.3 to 7 ka (Table S1). Most important for assigning a minimum age to the human hand and footprints is the oldest generation of pore cements, i.e. a dense, clean and laminated calcite for which four sub-samples from three travertine samples (all adjacent to the imprints) yielded a weighted mean age of 7.4 ± 0.1 ka.(Fig. 2). ^{230}Th/U ages from samples obtained further down-section (a dense travertine sample from 6.6 m and a flowstone sample that precipitated in a fracture at 7.6 m below the imprints; Fig. 2) increase with depth and are thus in stratigraphic order.

For optical dating, sand-sized quartz grains were extracted from the three travertine samples collected from the imprinted travertine sheet. Only one sample (CS-T-2) yielded enough quartz for dating. A single-grain approach was used for paleodose (De) estimation in order to investigate partial bleaching *(19)*. Determination of the environmental dose rate was aided by modelling to handle disequilibria in the radioisotope decay chains and to constrain the effect of different burial scenarios on the OSL age *(19)* (Fig. S6, Tables S2-3). The single-grain De distribution is 37% overdispersed

(Fig. S6) and petrographic thin section analysis reveal a clastic micro-fabric for sample CS-T-2 (rounded to sub-angular travertine clasts that are suggestive of short transport distances; Fig. S5). Both observations suggest that the OSL signals of these quartz grains were incompletely reset during transport (i.e. partially bleached) and that a minimum age model is appropriate for De calculation (20). Combining the minimum De value of sample CS-T-2 with the minimum and maximum dose rate scenarios constrains the age of the imprinted travertine sheet to ca. 10 – 14 ka (Fig. 2).

Radiocarbon dating was conducted on both the bulk sediment and on microscopic plant remains of two colluvial sediment samples and one clastic but organically rich travertine sample. For the bulk sediment dating fractions radiocarbon ages were obtained via the ABA and ABOxA pretreatment techniques, while the microbotanic dating fractions have been ABA pretreated only (19). The organically rich colluvium layer from a stratigraphic position directly below the imprints (Dms #1, Fig. 2) yielded ages of ca. 8.20-8.36 and 8.37-8.51 ka cal. BP for the ABA pretreated bulk and microbotanic fractions, respectively (Table S4, Fig. S7). The ABOxA age on the bulk dating fraction of the same colluvium layer is significantly older (ca. 12.67-12.75 ka cal. BP), but for methodological reasons may not be accurate (19). Radiocarbon ages increase down-section and broadly confirm the [230]Th/U ages from 7.4 m depth (11.4 ± 0.5 ka) and 8.1 m depth (> 13.3 ± 0.14 ka) and thus constrain the depositional history of the lower part of this travertine-colluvium succession to the Latest Pleistocene (Fig. 2, Table S4).

The palynological data were obtained discontinuously along the stratigraphic profile and are best understood as paleoecological snapshots providing insights into three discrete time-slices at ca. 15 ka, 11 ka and 8.4 ka, respectively (19). In each, non-arboreal pollen predominates, suggesting that the landscape during the Latest Pleistocene and Early Holocene was characterized by an alpine steppe dominated by wormwood (*Artemisia*) and grasses (Poaceae; Fig. S8). The palynological data do not support the presence of regional tree resources, but indicate the presence of local shrubs (i.e. *Hippophae*/seabucksthorn) and megaherbivores.

No artifacts were found near the travertine sheet with the embedded prints. Extensive pedestrian survey of the area surrounding the hot springs located two low-density concentrations of reduction by-products: Localites A and B (Fig. S9 A-O). These lithics reflect core-flake and blade-core technologies that are consistent with materials found in assemblages thought to date to the Late Paleolithic or Early Holocene on the northeastern margin of the plateau (10, 21, 22). No microlithic tools or ceramics, which are generally indicative of mid-to-late Holocene occupations (6), are found at Chusang.

Although the geochronology of the site is complex, these lines of evidence show that the minimum age of the Chusang site, as dated by a consistent set of [230]Th/U ages taken from a single generation of clean pore cement postdating the prints, is 7.4 ± 0.1 ka. Although we cannot state with certainty a maximum age for the site, we can offer two alternatives: (i) the maximum age of the prints is constrained by ^{14}C assays to ca. 8.20-8.51 ka cal. BP from the colluvium immediately below the travertine sheet or (ii) a maximum age of ca. 12.7 ka cal. BP, which is consistent with the OSL dates on travertine that range in date from 10.0-14.0 ka. For either scenario, these dates make Chusang the oldest reliably dated archaeological site on the high elevation step of the Tibetan plateau.

This finding has important implications for evaluating current models of the peopling of the plateau. To be a station (23) or task-specific site monitored seasonally from a base camp at a lower elevation (<3300m), travel costs would have been considerable. Travel cost modelling shows that round-trip travel times from such a base camp would have minimally required 28-47 days (19) (Fig.

S10_2A). However, this route must cross the Eastern Himalayan range and would have been impassable for much of the year – especially during the Early Holocene – due to the closure of high passes by heavy snowfall and expansion of valley glaciers in response to increased precipitation from the Indian summer monsoon (*9, 24*). A more plausible route (Fig. S10_2B) from the southeast shows a round-trip travel time of 41-70 days. Such travel is unlikely to have been undertaken for seasonal, short-term task pursuits in rugged, mountainous terrain, particularly by age-variable groups that may have included children, as is suggested by the presence of small footprints at Chusang (*17, 25*). These estimates also exceed annual travel distances for most ethnographically known foraging peoples (*26, 27*). Instead, the data from Chusang support a model of an annual settlement pattern focused upon the high interior plateau that likely utilized adjacent valleys of the major river courses at elevations above 3600 masl. While we cannot entirely rule out the possibility of logistical use of Chusang by low-elevation foragers, our analyses of archaeological, geographic, demographic, environmental, and ethnographic evidence converge to suggest that this type of use was highly improbable.

The data from Chusang support the presence of an early, pre-agropastoral population of the high elevation step of the Tibetan plateau at ca. 7.4-8.4 ka, although an earlier presence at ca. 12-13 ka cannot be fully discounted. These dates are consistent with what is known of the ancestral genetics of modern Tibetans (*11-15*) and coincide with wet and humid climate conditions on the Tibetan Plateau that lasted from ca. 11.5 ka until 4.2 ka due to an enhanced Indian summer monsoon (*28-30*). Although an agro-pastoral lifeway may have enabled significant population growth after 5 ka, it by no means was required for the early, likely permanent, occupation of the high central valleys of the Tibetan plateau.

References and Notes:

1. F. H. Chen et al., Agriculture facilitated permanent human occupation of the Tibetan Plateau after 3600 BP. *Science* **347**, 248–250 (2015).
2. M. Aldenderfer, Peopling the Tibetan Plateau: insights from archaeology. *High Alt. Med. Biol*. **12**, 141–147 (2011).
3. P.J. Brantingham, D. Rhode, D. Madsen, Archaeology augments Tibet's genetic history. *Science* **329**, 1467 (2010).
4. L. Barton, The cultural context of biological adaptation to high elevation Tibet. *Arch. Res. Asia* **5**, 4-11 (2016).
5. D. Madsen, Conceptualizing the Tibetan Plateau: environmental constraints on the peopling of the "Third Pole". *Arch. Res. Asia* **5**, 24-32 (2016).
6. M. Aldenderfer, Y. Zhang, The prehistory of the Tibetan Plateau to the seventh century A.D.: perspectives and research from China and the West since 1950. *J. World Prehist*. **18**, 1–55 (2004).
7. P.J. Brantingham *et al*., "A short chronology for the peopling of the Tibetan Plateau" in *Developments in Quaternary Science: Late Quaternary Climate Change and Human Adaptation in Arid China*, D.B. Madsen, F.H. Chen, G. Xing, Eds. (Elsevier, Amsterdam, 2007), vol. 9, pp. 129-150.
8. D.B. Madsen, F.H. Chen, G. Xing, "Changing views of Late Quaternary human adaptation in arid China" in *Developments in Quaternary Science: Late Quaternary Climate Change and Human Adaptation in Arid China*, D.B. Madsen, F.H. Chen, G. Xing, Eds. (Elsevier, Amsterdam, 2007), vol. 9, pp. 227-232.
9. M.C. Meyer, R. A. Cliff, C. Spötl, M. Knipping, A. Mangini, Holocene glacier fluctuations and migration of Neolithic yak pastoralists into the high valleys of northwest Bhutan. *Quat. Sci. Rev.* **28**, 1217–1237 (2009).
10. P.J. Brantingham *et al.,* Late occupation of the high-elevation northern Tibetan Plateau based on cosmogenic, luminescence, and radiocarbon ages*. Geoarchaeology* **28**, 413–431 (2013).

11. Z. Qin *et al.,* A mitochondrial revelation of early human migrations to the Tibetan Plateau before and after the Last Glacial Maximum. *Am. J. Phys. Anthropol.* **143**, 555–569 (2010).

12. M. Zhao *et al.,* Mitochondrial genome evidence reveals successful Late Paleolithic settlement on the Tibetan Plateau. *Proc. Natl. Acad. Sci U.S.A.* **106**, 21230–21235 (2009).

13. K. Xiang *et al.,* Identification of a Tibetan-specific mutation in the hypoxic gene EGLN1 and its contribution to high-altitude adaptation. *Mol. Biol. Evol.* **30**, 1889-1898 (2013).

14. F. Lorenzo *et al.*, A genetic mechanism for Tibetan high-altitude adaptation. *Nature Genet.* **46**, 951-956 (2014).

15. X. Qi *et al.*, Genetic evidence of paleolithic colonization and Neolithic expansion of modern humans on the Tibetan Plateau. *Mol. Biol. Evol.* **30**, 1761-1778 (2013).

16. D.D. Zhang, S.H. Li, Optical dating of Tibetan human hand- and footprints: an implication for the palaeoenvironment of the last glaciation of the Tibetan Plateau. *Geophys. Res. Lett.* **29**, 1072 (2002).

17. D.D. Zhang, S. H. Li, Y. Q. He, B. S. Li, Human settlement of the last glaciation on the Tibetan Plateau. *Curr. Sci.* (India) **84**, 701–704 (2003).

18. Z. Wang, M.C. Meyer, D.L. Hoffmann, Sedimentology, petrography and early diagenesis of a travertine–colluvium succession from Chusang (southern Tibet). *Sediment. Geol.* **342**, 218-236 (2016).

19. Material and Methods are available as supplementary online materials on Science Online

20. G.A.T. Duller, Single-grain optical dating of Quaternary sediments: why aliquot size matters in luminescence dating. *Boreas* **37**, 589–612 (2008).

21. S. Pei *et al,* The Shuidonggou site complex: new excavations and implications for the earliest Late Paleolithic in North China. *J. Arch. Sci.* **39**, 3610–3626 (2012).

22. P.J. Brantingham, J. W. Olsen, G. B. Schaller, Lithic assemblages from the Chang Tang region, Northern Tibet. *Antiquity* **75**, 319–327 (2001).

23. R. Bettinger, R. Garvey, S. Tushingham, *Hunter-gatherers: Archaeological and Evolutionary Theory* (Springer, New York, 2015).

24. L.A. Owen, Latest Pleistocene and Holocene glacier fluctuations in the Himalaya and Tibet. *Quat. Sci. Rev.* **28**, 2150–2164 (2009).

25. M. Aldenderfer, *Montane Foragers* (Univ. Iowa Press, Iowa City IA, 1998).

26. R. Kelly, Hunter-gatherer mobility strategies. *J. Anthropol. Res.* **39**, 277–306 (1983).

27. R. Kelly, *The Foraging Spectrum* (Percheron Press, Clinton Corners, NY, 2007).

28. Y. Cai *et al.,* The Holocene Indian monsoon variability over the southern Tibetan Plateau and its teleconnections. *Earth Planet. Sci. Lett.* **335-336**, 135-144 (2012).

29. D. Fleitmann *et al.,* Holocene ITCZ and Indian monsoon dynamics recorded in stalagmites from Oman and Yemen (Socotra). *Quat. Sci. Rev.* **26**, 170–188 (2007).

30. L. Zhu *et al.,* Climate change on the Tibetan Plateau in response to shifting atmospheric circulation since the LGM. *Sci. Rep.* **5**, 13318 (2015).

_____here the supplement starts_____

31. N. Eyles, C.H. Eyles, A.D. Miall, Lithofacies types and vertical profile models - an alternative approach to the description and environmental interpretation of glacial diamict and diamictite sequences. *Sedimentology* **30**, 393-410 (1983).

32. B. Jones, R.W. Renaut, R.B. Owen, H. Torfason, Growth patterns and implications of complex dendrites in calcite travertines from Lýsuhóll, Snæfellsnes, Iceland. *Sedimentology* **52**, 1277-1301 (2005).

33. B. Jones, R.W. Renaut, Cyclic development of large, complex, calcite dendrite crystals in the Clinton travertine, Interior British Columbia, Canada. *Sediment. Geol.* **203**, 17-35 (2008).

34. L. Guo, R. Riding, Hot-spring travertine facies and sequences, Late Pleistocene, Rapolano Terme, Italy. *Sedimentology* **45**, 163-180 (1998).

35. D.K. Rainey, B. Jones, Abiotic versus biotic controls on the development of the Fairmont Hot Springs carbonate deposit, British Columbia, Canada. *Sedimentology* **56**, 1832-1857 (2009).

36. M. Özkul *et al.*, Sedimentological and geochemical characteristics of a fluvial travertine: A case from the eastern Mediterranean region. *Sedimentology* **61**, 291-318 (2014).

37. A. Heimann, E. Sass, Travertines in the northern Hula Valley, Israel. *Sedimentology* **36**, 95-108 (1989).
38. A. Pentecost, *Travertine* (Springer, Berlin, 2005).
39. Z.H. Liu *et al.*, Wet-dry seasonal variations of hydrochemistry and carbonate precipitation rates in a travertine-depositing canal at Baishuitai, Yunnan, SW China: Implications for the formation of biannual laminae in travertine and for climatic reconstruction. *Chem. Geol.* **273**, 258-266 (2010).
40. H.S. Chafetz, S.A. Guidry, Deposition and diagenesis of Mammoth Hot Springs travertine, Yellowstone National Park, Wyoming, USA. *Can. J. Earth Sci.* **40**, 1515-1529 (2003).
41. D.G. Sanders, M. Ostermann, J. Kramers, Meteoric diagenesis of Quaternary carbonate-rocky talus slope successions (Northern Calcareous Alps, Austria). *Facies* **56**, 27-46 (2010).
42. D.L. Hoffmann, Th-230 isotope measurements of femtogram quantities for U-series dating using multi ion counting (MIC) MC-ICPMS. *Int. J. Mass Spectrom.* **275**, 75-79 (2008).
43. D.L. Hoffmann *et al.*, Procedures for accurate U and Th isotope measurements by high precision MC-ICPMS. *Int. J. Mass Spectrom.* **264**, 97-109 (2007).
44. A.H. Jaffey, K.F. Flynn, L.E. Glendenin, W.C. Bentley, A.M. Essling, Precision measurement of half-lives and specific activities of U-235 and U-238. *Phys. Rev. C* **4**, 1889-1906 (1971).
45. H. Cheng *et al.*, The half-lives of uranium-234 and thorium-230. *Chem. Geol.* **169**, 17-33 (2000).
46. N.E. Holden, Total half-lives for selected nuclides. *Pure Appl. Chem.* **62**, 941-958 (1990).
47. K.H. Wedepohl, The composition of the continental-crust. *Geochim. Cosmochim. Acta* **59**, 1217-1232 (1995).
48. A.G. Wintle, Luminescence dating: Laboratory procedures and protocols. *Radiat. Meas.* **27**, 769-817 (1997).
49. L. Bøtter-Jensen, E. Bulur, G.A.T. Duller, A.S. Murray, Advances in luminescence instrument systems. *Radiat. Meas.* **32**, 523-528 (2000).
50. A.S. Murray, A.G. Wintle, Luminescence dating of quartz using an improved single-aliquot regenerative-dose protocol. *Radiat. Meas.* **32**, 57-73 (2000).
51. G.A.T. Duller, Distinguishing quartz and feldspar in single grain luminescence measurements. *Radiat. Meas.* **37**, 161-165 (2003).
52. Z. Jacobs, G.A.T. Duller, A.G. Wintle, Optical dating of dune sand from Blombos Cave, South Africa: II - single grain data. *J. Hum. Evol.* **44**, 613-625 (2003).
53. S. Niese, M. Koehler, B. Gleisberg, Low-level counting techniques in the underground laboratory "Felsenkeller" in Dresden. *J. Radioanal. Nucl. Chem.* **233**, 167-172 (1998).
54. G. Guérin, N. Mercier, G. Adamiec, Dose-rate conversion factors: update. *Ancient TL* **29**, 5-8 (2011).
55. B.J. Brennan, Beta dose to spherical grains. *Radiat. Meas.* **37**, 299-303 (2003).
56. B.J. Brennan, R.G. Lyons, S.W. Phillips, Attenuation of alpha particle track dose for spherical grains. *Int. J .Rad. Appl. Instrum. D* **18**, 249-253 (1991).
57. DDEP, http://laraweb.free.fr/, requested February 2016.
58. J.R. Prescott, J.T. Hutton, Cosmic ray contributions to dose rates for luminescence and ESR dating: Large depths and long-term time variations. *Radiat. Meas.* **23**, 497-500 (1994).
59. J.R. Prescott, J.T. Hutton, Cosmic ray and gamma ray dosimetry for TL and ESR. *Int. J. Rad. Appl. Instrum. D* **14**, 223-227 (1988).
60. G. Kulig, "Erstellung einer Auswertesoftware zur Altersbestimmung mittels Lumineszenzverfahren unter spezieller Berücksichtigung des Einflusses radioaktiver Ungleichgewichte in der ^{238}U-Zerfallsreihe", Bachelor thesis, TU Bergakademie Freiberg (2005).
61. D. Degering, G. Kulig, M. Krbetschek, "ADELE - a novel software for age determination based on luminescence and electron spin resonance", poster in *11th Conference on Luminescence and Electron Spin Resonance Dating*, Cologne, Germany, 24–29 July 2005.
62. M.J. Aitken, *Thermoluminescence Dating. Studies in archaeological sciences* (Academic Press, London, 1985).
63. G.A.T. Duller, The Analyst software package for luminescence data: overview and recent improvements. *Ancient TL* **33**, 35-42 (2015).
64. R.M. Bailey, B.W. Smith, E.J. Rhodes, Partial bleaching and the decay form characteristics of quartz OSL. *Radiat. Meas.* 27, 123-136 (1997).

65. R.F. Galbraith, R.G. Roberts, G.M. Laslett, H.Yoshida, J.M. Olley, Optical dating of single grain and multiple grains of quartz from Jinmium rock shelter, Northern Australia: part I, experimental design and statistical models. *Archaeometry* **41**, 339-364 (1999).

66. L. Plan, Factors controlling carbonate dissolution rates quantified in a field test in the Austrian alps. *Geomorphology* **68,** 201-212 (2005).

67. P. Häuselmann, Surface corrosion of an Alpine karren field: recent measures at Innerbergli (Siebenhengste, Switzerland). *Int. J. Speleol.* **37**, 107-111(2008).

68. S. Furlani, F. Cucchi, F. Froti, A. Rossi, Comparison between coastal and inland Karst limestone lowering rates in the northeastern Adriatic Region (Italy and Croatia). *Geomorphology* **104**, 73-81 (2009).

69. M. Ivanovich, R.S. Harmon, *Uranium-series Disequilibrium: Applications to Earth, Marine, and Eenvironmental Sciences* (Clarendon Press, Oxford ed. 2, 1992).

70. A. Zander, D. Degering, F. Preusser, H.U. Kasper, H. Bruckner, Optically stimulated luminescence dating of sublittoral and intertidal sediments from Dubai, UAE: radioactive disequilibria in the uranium decay series. *Quat. Geochronol.* **2**, 123-128 (2007).

71. N.C. Sturchio, Radium isotopes, alkaline-Earth diagenesis, and age-determination of travertine from Mammoth hot-springs, Wyoming, USA. *Appl. Geochem.* **5**, 631-640 (1990).

72. A. Onishchenko, M. Zhukovsky, N. Veselinovic, Z.S. Zunic, Radium-226 concentration in spring water sampled in high radon regions. *Appl. Radiat. Isot.* **68**, 825-827 (2010).

73. M. Stuiver, H. A. Polach, Discussion: reporting of ^{14}C data. *Radiocarbon* **19**, 355–363 (1977).

74. D.J. Donahue, T.W. Linick, A.J.T. Jull, Isotope-ratio and background corrections for accelerator mass spectrometry radiocarbon measurements. *Radiocarbon*, **32**(2), 135-142 (1990).

75. P.J. Reimer et al., IntCal13 and Marine13 radiocarbon age calibration curves 0–50,000 years cal BP. *Radiocarbon* **55**, 1869-1887 (2013).

76. M. Stuiver, J. Reimer, Extended ^{14}C data base and revised CALIB 3.0 ^{14}C age calibration program. *Radiocarbon* **35**, 215-30 (1993).

77. J.C. Turnbull et al., High-precision atmospheric [14]CO$_2$ measurement at the Rafter Radiocarbon Laboratory. *Radiocarbon* **57**(3), 377-388 (2015).

78. C. Hatté, J. Morvan, C.Noury, M. Paterne, Is classical acid-alkali-acid treatement responsible for contamination? An alternative proposition. *Radiocarbon* **43**, 177-182 (2001).

79. I. Hajdas, Radiocarbon dating and its applications in Quaternary studies. *E&G – Quat. Sci. J.* **57**, 2-24 (2008).

80. R. Gillespie, On the use of oxidation for AMS sample pretreatment. *Nucl. Instr. Meth. Phys. Res. B* **52**, 345-347 (1990).

81. M.I. Bird *et al.*, The efficiency of charcoal decontamination for radiocarbon dating by three pre-treatments - ABOX, ABA and hypy. *Quat. Geochronol.* **22**, 25-32 (2014).

82. M.I. Bird, *Charcoal*. In: S.A. Elias, Ed. *The Encyclopedia of Quaternary Science* (Elsevier, Amsterdam, 2013), vol. 4, pp. 353-360.

83. C. Carcaillet, Are Holocene wood-charcoal fragments stratified in alpine and subalpine soils? Evidence from the Alps based on AMS ^{14}C dates. *The Holocene* **11**, 231–242 (2001).

84. M.S. Hopkins, A.W. Graham, R. Hewett, J. Ash, J. Head, Evidence of late Pleistocene fires and eucalypt forest from a north Queensland humid tropical rainforest site. *Aust. J. Ecol.* **15**, 345–347 (1990).

85. L.C.R. Pessenda, S.E.M. Gouveia, R. Aravena, Radiocarbon dating of total soil organic matter and humin fraction and its comparison with ^{14}C ages of charcoal. *Radiocarbon* **43**, 595–601 (2001).

86. R.J. Blong, R. Gillespie, Fluvially transported charcoal gives erroneous ^{14}C ages for recent deposits. *Nature* **271**, 739-741 (1978).

87. T.E. Törnqvist, A.F. de Jong, W.A. Oosterbaan, K. Van der Borg, Accurate dating of organic deposits by AMS 14C measurement of macrofossils. *Radiocarbon* **34**(3), 566-577 (1992).

88. T. Higham *et al.*, Problems with radiocarbon dating the Middle to Upper Palaeolithic transition in Italy. *Quat. Sci. Rev.* **28**(13), 1257-1267 (2009).

89. G. Santos, K. Ormsby, Behavioral variability in ABA chemical pretreatment close to the ^{14}C age limit. *Radiocarbo*n **55**(534-544) (2013).

90. R. Gillespie, Burnt and unburnt carbon: dating charcoal and burnt bone from the Willandra Lakes, Australia. *Radiocarbon* **39**(3), 239-250 (1997).

91. M.I. Bird *et al.*, Radiocarbon dating of "old" charcoal using a wet oxidation, stepped-combustion procedure. *Radiocarbo*n **41**(2), 127-14 (1999).

92. C.S.M. Turney *et al.*, Development of a robust ^{14}C chronology for Lynch's Crater (North Queensland, Australia): using different pretreatment strategies. *Radiocarbon* **43**(1), 45-54 (2001).

93. W. Zhou, D. Donahue, A.J.T. Jull, Radiocarbon AMS dating of pollen concentrated from eolian sediments: implications for monsoon climate change since the late Quaternary. *Radiocarbon* **39**(1), 19-26 (1997).

94. H.-J. Beug, G. Miehe, Vegetation history and human impact in the eastern Central Himalaya (Langtang and Helambu, Nepal), *Dissertationes Botanicae* **318**, 1-98 (1999).

95. F. Wang, N. Chien, Y. Zhang, H. Yang, *Pollen Flora of China (in Chinese)* (Science Press, Beijing, 1995).

96. Q. Xu, *China Commonly Cultivated Pollen Morphology* (Science Press, Beijing, 2015).

97. B. van Geel, A. Aptroot, Fossil ascomycetes in Quaternary deposits, *Nova Hedwigia* **82**, 313-330 (2006).

98. H.-J. Beug, *Leitfaden der Pollenbestimmung für Mitteleuropa und angrenzender Gebiete* (Pfeil, München, 2004).

99. U. Herzschuh, H. Kürschner, S. Mischke, Temperature variability and vertical vegetation belt shifts during the last ~50,000 yr in the Qilian Mountains (NE margin of the Tibetan Plateau, China), *Quat. Res.* **66**, 133-146 (2006).

100. G. Miehe *et al.,* How old is Pastoralism in Tibet? An Ecological Approach to the Making of a Tibetan Landscape, *Palaeogeogr. Palaeoclimatol. Palaeoecol.* **276**, 130–147 (2009).

101. F. Schlütz, F. Lehmkuhl, Holocene climatic change and the nomadic Anthropocene in Eastern Tibet: Palynological and geomorphological results from the Nianbaoyeze Mountains, *Quat. Sci. Rev.* **28**, 1449-1471 (2009).

102. W. Tobler, "Three Presentations on Geographical Analysis and Modeling" (Technical Report 93–1, National Center for Geographic Information and Analysis, Santa Barbara, 1993).

103. A.E. Minetti, C. Moia, G.S. Roi, D. Susta, G. Ferretti, Energy cost of walking and running at extreme uphill and downhill slopes. *J. Appl. Physiol.* **93**, 1039-1046 (2002).

104. J.J. Danielson, D.B. Gesch, "Global Multi-resolution Terrain Elevation Data 2010 (GMTED2010)" (Open-File Report 2011-1073, U.S. Geological Survey, 2011), p. 26.

105. E.W. Dijkstra, A note on two problems in connexion with graphs. *Numer. Math.* **1**, 269-271 (1959).

106. R Core Team, *R: A Language and Environment for Statistical Computing* (R Foundation for Statistical Computing, Vienna, Austria, 2013; http://www.R-project.org/).

107. R. Bivand, E. J. Pebesma, V. Gómez-Rubio, *Applied spatial data analysis with R* (Springer, New York, 2nd ed., 2013), *Use R!*

108. R.J. Hijmans, *raster: Geographic Data Analysis and Modeling* (2015; https://CRAN.R-project.org/package=raster), *R Package*.

109. J. van Ettan, R Package gdistance: distances and routes on geographical grids. *J. Stat. Softw.* **VV** (2016).

110. C.M. Beall, Adaptation to high altitude: phenotypes and genotypes. *Annu. Rev. Anthropol.* **43**, 251-412 (2014).

Supplementary Materials:

Supplementary Text S1
Materials and Methods
Figures S1 to S10
Tables S1 to S5
References (31–110)

Figure Captions:

Figure 1: The Tibetan Plateau and Paleolithic sites with absolute age control (> 10 kyr cal. BP, circles) or a tentative Paleolithic age assocation (rectangles) based on typological cross-dating of lithic artefacts with sites of known age. Sites (Q = Qinghai sites): 1, Chusang; 2, Su-re; 3, Ha-dong-tang & Que-de-tang; 4, Zhu-luo-le; 5, Siling-co; 6, Duo-ge-ze; 7, Ge-ting; 8, Zha-bu; 9, Xia-da Co; 10, Re-jiao; 11, Gong-ben; Q1, Xiao Qaidam; Q2, Heimahe 1; Q3, Jiangxigou 1; Q4, Lenghu 1; Q5, Wulanwula Lake; Q6, Yeniugou; Q7, Bronze Wine Canyon; Q8, Ten Hearths.

Figure 2: Stratigraphic profile of the Chusang travertine with position of human hand and footprints and absolute age control. Trav. = Travertine, Dms = diamict massive stratified (colluvium composed of debris flows), cmt. = carbonate cemented, +org. = containing organic matter. Horizontal axis indicates grain size distribution. Radiocarbon ages in square brackets are further discussed in (19).

Figure 3: Well preserved human footprints visualized via a 3D model (A) and corresponding field image (B). The annual travertine layers below these imprints are bended (C), suggestive of human presence during Chusang travertine formation. The porous summer layers contain numerous cement generations that precipitated shortly after travertine deposition. For the laminated pore cement a ^{230}Th/U age of 7.4 ka was obtained, providing a robust minimum age for the imprints.
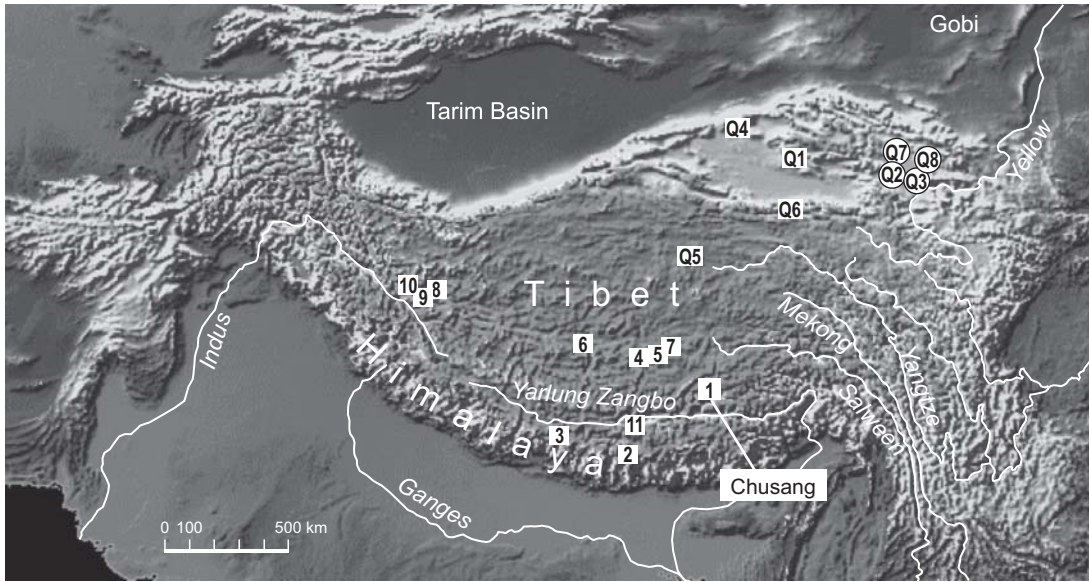
Figure 1

Figure 2

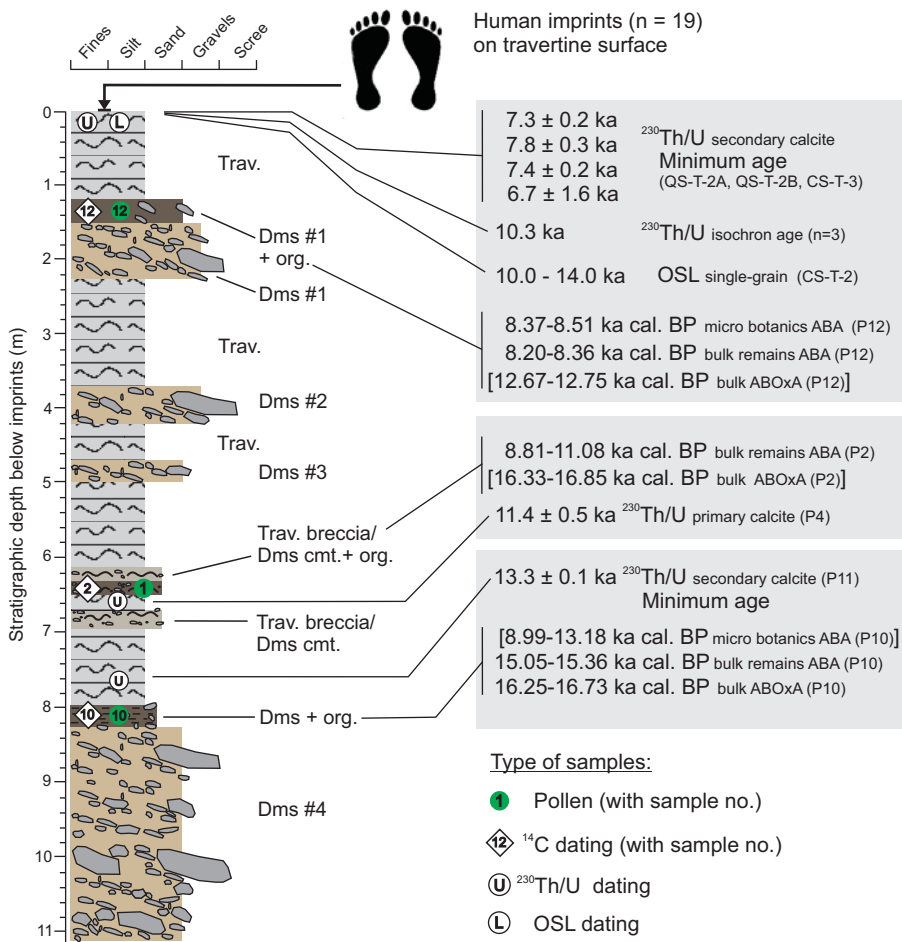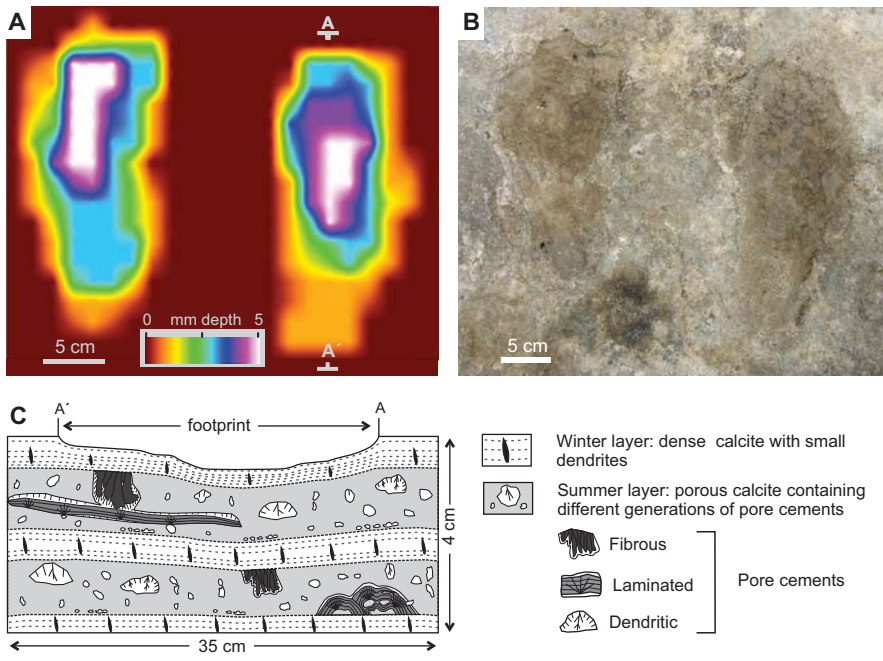Figure 3